



Universiteit
Leiden
The Netherlands

Light transmittance in human atrial tissue and transthoracic illumination in rats support translatability of optogenetic cardioversion of atrial fibrillation

Nyns, E.C.A.; Portero, V.; Deng, S.L.; Jin, T.Y.; Harlaar, N.; Bart, C.I.; ... ; Pijnappels, D.A.

Citation

Nyns, E. C. A., Portero, V., Deng, S. L., Jin, T. Y., Harlaar, N., Bart, C. I., ... Pijnappels, D. A. (2023). Light transmittance in human atrial tissue and transthoracic illumination in rats support translatability of optogenetic cardioversion of atrial fibrillation. *Journal Of Internal Medicine*. doi:10.1111/joim.13654

Version: Publisher's Version

License: [Creative Commons CC BY-NC-ND 4.0 license](https://creativecommons.org/licenses/by-nc-nd/4.0/)

Downloaded from: <https://hdl.handle.net/1887/3633620>

Note: To cite this publication please use the final published version (if applicable).

Light transmittance in human atrial tissue and transthoracic illumination in rats support translatability of optogenetic cardioversion of atrial fibrillation

■ Emile C. A. Nyns¹, Vincent Portero¹, Shanliang Deng¹, Tianyi Jin², Niels Harlaar¹, Cindy I. Bart¹, Thomas J. van Brakel³, Meindert Palmen³, Jesper Hjortnaes³, Arti A. Ramkisoensing¹, Guo Qi Zhang², René H. Poelma², Balázs Ördög¹, Antoine A. F. de Vries¹ & Daniël A. Pijnappels¹ 

From the ¹Laboratory of Experimental Cardiology, Department of Cardiology, Leiden University Medical Center (LUMC), Leiden, the Netherlands; ²Department of Microelectronics, Delft University of Technology, Delft, the Netherlands; and ³Department of Cardiothoracic Surgery, LUMC, Leiden, the Netherlands

Abstract. Nyns ECA, Portero V, Deng S, Jin T, Harlaar N, Bart CI, et al. Light transmittance in human atrial tissue and transthoracic illumination in rats support translatability of optogenetic cardioversion of atrial fibrillation. *J Intern Med.* 2023;00:1–11.

Background. Optogenetics could offer a solution to the current lack of an ambulatory method for the rapid automated cardioversion of atrial fibrillation (AF), but key translational aspects remain to be studied.

Objective. To investigate whether optogenetic cardioversion of AF is effective in the aged heart and whether sufficient light penetrates the human atrial wall.

Methods. Atria of adult and aged rats were optogenetically modified to express light-gated ion channels (i.e., red-activatable channelrhodopsin), followed by AF induction and atrial illumination to determine the effectivity of optogenetic cardiover-

sion. The irradiance level was determined by light transmittance measurements on human atrial tissue.

Results. AF could be effectively terminated in the remodeled atria of aged rats (97%, $n = 6$). Subsequently, ex vivo experiments using human atrial auricles demonstrated that 565-nm light pulses at an intensity of 25 mW/mm² achieved the complete penetration of the atrial wall. Applying such irradiation onto the chest of adult rats resulted in transthoracic atrial illumination as evidenced by the optogenetic cardioversion of AF (90%, $n = 4$).

Conclusion. Transthoracic optogenetic cardioversion of AF is effective in the aged rat heart using irradiation levels compatible with human atrial transmural light penetration.

Keywords: arrhythmia, atrial fibrillation, gene therapy, optogenetics, translational research

Introduction

Despite treatment advances for atrial fibrillation (AF), many patients continue to experience frequent AF recurrences. This puts them at an increased risk for mortality, morbidity, and impaired quality-of-life given the progressive nature of AF (i.e., AF begets AF) and the current lack of therapeutic strategies to sustain sinus rhythm in a safe, continuous, and effective man-

ner [1–3]. Although implantable atrial cardioverters have been shown to be capable of safe and effective rhythm control in an ambulatory setting, their use was never adopted in routine clinical practice because of severe pain caused by electroshocks in conscious patients [4, 5]. Recently, a novel therapeutic approach enabling automated shock-free termination of AF has been developed and successfully demonstrated in a closed-chest animal model

through bioelectronic engineering [6]. Such shock-free AF termination was realized by the appropriately timed generation of endogenous cardiac currents after forced expression and subsequent activation of light-gated ion channels, a technique that is referred to as optogenetics [7, 8]. Automated arrhythmia-triggered activation of an implanted light source facing the atrial epicardium of the optogenetically modified adult rat resulted in the safe, effective, continuous yet shock-free restoration of sinus rhythm [6], thereby raising the perspective of pain-free ambulatory rhythm control in patients with symptomatic AF. Although the current preclinical results of the optogenetic termination of AF seem promising, there is uncertainty regarding the clinical potential because its feasibility has not been tested in structurally and electrically remodeled atria, which is the typical setting in which AF occurs. In addition, it is currently unknown whether optogenetic excitation light can penetrate the human heart deep enough for effective arrhythmia termination. We therefore evaluated, for the first time, the feasibility and effectiveness of optogenetic AF termination in aged rats with structural and electrical remodeled atria. In addition, we investigated light penetration through the human atrial wall in conjunction with animal experiments using transthoracic illumination protocols in order to explore the clinical feasibility of optogenetic AF termination.

Methods

Additional methods can be found in the Supporting Information section.

Study approval

All animal experiments were approved by the Animal Experiments Committee of Leiden University Medical Center (AVD1160020172929) and conformed to EU Directive 2010/63. This study was conducted with the approval of the institutional review board of the Leiden University Medical Center (P13.043) and in compliance with the International Code of Medical Ethics of the World Medical Association.

Human atrial samples and light penetration measurements

Human left atrial appendages resected during cardiac surgery were retrieved, after the heart was arrested with high potassium warm blood cardioplegia, in cold (4°C) phosphate-buffered saline

(PBS). These appendages were removed on clinical indication and collected in an anonymized fashion, as approved by the local ethics committee (protocol P13.043). Transmural tissue samples (generally measuring approximately $10 \times 10 \text{ mm}^2$) were embedded in 4% low melting point agarose (Sigma-Aldrich) in PBS. Embedded samples were fixed to the sample holder of the vibratome (VT1200S, Leica Microsystems) using Histoacryl (B. Braun), subsequently covered in cold (4°C) PBS and sectioned into 0.5- to 2.0-mm thick tissue slices using ceramic injector blades (Cadence). Samples were always cut in a longitudinal fashion. Slices were placed on a glass coverslip placed directly on top of an optical power meter (PM100D, Thorlabs) equipped with an S130C slim dual range sensor. Illumination of these slices was performed using a mounted 565-nm light-emitting diode (LED; M565L3, Thorlabs) with an adjustable collimation lens (COP1-A, Thorlabs) at varying light intensities (0.05–3.0 mW/mm²). Transmittance was calculated for each sample as the average measured irradiance underneath the tissue as a fraction of transmittance through an empty glass coverslip. Transmittance was measured four times for tissue slices from five patients of four different thicknesses—that is, a total of 80 individual measurements were performed. Transmittance from the atrial tissue surface was fitted using the Beer–Lambert law $T(D) = e^{-uD}$, in which D is the thickness of the tissue, and u is the attenuation coefficient of 565-nm light. The attenuation depth is the reciprocal of the attenuation coefficient ($1/u$). Fitting of the experimental data was performed using the Curve Fitting Toolbox (MATLAB R2019a, MathWorks) and yielded a coefficient of determination $R^2 > 0.87$.

Animal experiments

Adult (7-week-old) and aged (2-year-old) female Wistar rats (Charles River Laboratories) received adeno-associated viral vectors (AAVVs) coding for red-activatable channelrhodopsin (ReaChR) [6] by tail vein injection (10^{13} genome copies per 100 g of animal bodyweight). Citrine-encoding AAVVs [6] (10^{13} genome copies per 100 g of animal bodyweight) were administered to adult rats for negative control experiments. Electrocardiographic (ECG) data were collected using an eight-channel PowerLab data acquisition device and recorded and analyzed using LabChart Pro software version 7 (both from ADInstruments). Rapamycin (3 mg/kg; LC Laboratories) was administered every other day

by intraperitoneal injections for 3 weeks. Four to six weeks after AAVV delivery, the feasibility and efficacy of optogenetic termination of AF were studied *in vivo*.

Open-chest AF induction and termination

Aged and adult rats were anesthetized, intubated, and mechanically ventilated by inhaling 2%–3% isoflurane in O₂ at 0.8 L/min. Adequate anesthesia was confirmed by the absence of reflexes. The right atrium (RA) was visualized following an incision of the fourth right intercostal space and subsequent rib spreading. Inducibility of sustained AF (>30 s) without pro-arrhythmic drugs was evaluated by electrical burst pacing of the RA (cycle length 20–30 ms) using an STG4002 stimulus generator with MC Stimulus II software (Multichannel Systems). Aged rats in which sustained AF (>30 s) could be reliably induced were included in the study (six out of eight rats). As sustained AF could not be induced solely by burst pacing in the adult rats, a single intraperitoneal injection of carbachol (50 µg/kg) was administered 15 min before the induction of AF by electrical burst pacing of the RA, and carbachol injections were repeated every 30 min. Following carbachol injections, sustained AF could be induced in all adult rats (four out of four in both the ReaChR and Citrine group). The RA was optically stimulated by the aforementioned LED, which was powered by a 1200-mA LED driver in trigger mode (LEDD1B T-Cube LED driver, Thorlabs) and controlled by an STG2004 stimulus generator (Multichannel Systems), positioned at approximately 5 cm from the heart. Irradiance was measured using the optical power meter mentioned above. Following induction of sustained AF, the RA was subjected to three consecutive light pulses of 500 ms with 500-ms intervals (irradiance: 1 mW/mm²). AF was considered to be optogenetically terminated if the arrhythmia stopped within 2 s following the start of the last light pulse. All control experiments were performed in an identical fashion. ECG recordings were acquired and analyzed as described earlier.

Closed-chest AF induction and termination

Closed-chest AF experiments were performed on adult rats expressing ReaChR or Citrine. Animals were anesthetized as described above. In order to keep the thoracic wall completely closed, AF was induced by transesophageal atrial burst pacing (cycle length: 20–30 ms, current: 4 mA) for 5 s using a modified clinical pacing catheter (two 1-

mm rings with an interelectrode spacing of 2 mm). Optogenetic stimulation was performed closed-chest with a modified LED device consisting of four LEDs placed on the shaven thoracic wall around the fourth intercostal space right. LED placement in ReaChR-expressing rats was optimized by finding the position with the lowest irradiance thresholds for transthoracic optogenetic pacing of the RA. As AF could not be induced in the adult rats, carbachol was administered in an identical fashion as described above. Following intraperitoneal carbachol injections, sustained AF could be induced in all adult rats (four out of four in the ReaChR group and four out of four in the Citrine group). Following the induction of sustained AF, the LED device was activated three times (500 ms light pulses with 500 ms intervals) using an irradiance of 25 mW/mm². AF was considered to be optogenetically terminated if the arrhythmia stopped within 2 s following the start of the last light pulse. Control experiments in Citrine-expressing adult rats were performed in an identical manner.

Electrophysiological measurements by optical voltage mapping

Hearts were excised and cannulated for the Langendorff perfusion as previously described [9] and loaded with 12.5 µM of the voltage-sensitive dye di-4-ANBDQBS (AAT Bioquest). Optical recordings of action potential propagation were made using a MiCAM ULTIMA-L imaging system (SciMedia). Bipolar electrodes were placed in the ventricles for ECG recording and connected to a PowerLab 15T acquisition device (AD Instruments) controlled by LabChart Pro software version 7. Specialized software was used for data analysis (BrainVision Analyzer 1101, Brain Vision). Action potential duration at 50% repolarization (APD₅₀) was determined during 5-Hz pacing at 20 different locations equally distributed throughout the right and left atria. APD₅₀ dispersion was defined as the maximal difference in APD₅₀ within the atria. The coefficient of variation was expressed as the standard deviation (SD) divided by the mean.

Electrophysiological experiments by sharp electrode measurements

Light-induced membrane potential changes were recorded from apical tissue by the conventional intracellular sharp electrode technique. The tissue was immobilized in the tissue bath and superfused with oxygenated normal Tyrode solution (mM: NaCl

126, KCl 5.4, MgCl₂ 1, CaCl₂ 1.8, Glucose 11, HEPES 10, pH7.4) supplemented with 20 mM of 2,3-butanedione 2-monoxime in order to prevent movement of the tissue due to contractions. Microelectrodes had resistances between 12 and 15 MΩ when filled with the internal solution containing 3 M KCl. Impalement was evaluated to be successful when resting potentials were more negative than -70 mV and action potentials triggered by an external stimulus generator could be observed. The tissue was then illuminated by 565-nm light for 500 ms at illumination intensities varying from 0.1 to 2 mW/mm², with a 10-s dark period between each light pulse. End-plateau potentials were measured at the end of the 500-ms light pulse and were included in the study only when obtained from the same impalement. Data acquisition and analysis were achieved by a MultiClamp 700B patch clamp amplifier, the Digidata 1440A digital-analog interface, and pCLAMP software (version 10.7, Molecular Devices). The light source comprised a LED M565L3, the COP1-A collimation adapter, and the LEDD1B LED driver and was controlled by the pCLAMP software using the analog output of the Digidata 1440A interface. Light was delivered by positioning the LED-collimation lens assembly above the tissue bath at an approximately 15 cm distance.

Construction of the LED device

A custom-made integrated LED device was designed and fabricated. The device consisted of four high-power LEDs (LUXEON Z LXZ1-PX01, Lumileds) and transparent layers of UV-curable optical polymer (NOA63, Norland Products). The four LEDs provided a constant color spectrum with peak wavelength $\lambda = 567$ nm (lime), and all LEDs were simultaneously controlled by an external LED driver (LEDD1B). The current could be continuously adjusted from 0 to the maximum rated values of the LEDs at 700 mA (2.85 W for each LED). The four LEDs were placed side-by-side to achieve a 2 × 2 arrangement (Fig. 1D). The anodes and cathodes of nearby LEDs were soldered by lead-free solder. The distance between the center of each LED was 1.3 mm. A transparent layer (center thickness 1.0 mm) of UV-curable optical polymer was applied on the front side of the LED arrangement to physically fix and electrically insulate the high-power LEDs. The curing was performed at room temperature under four UV lamps (Cleo Compact 15W, Philips) for 10 min. The input anode and input cathode were

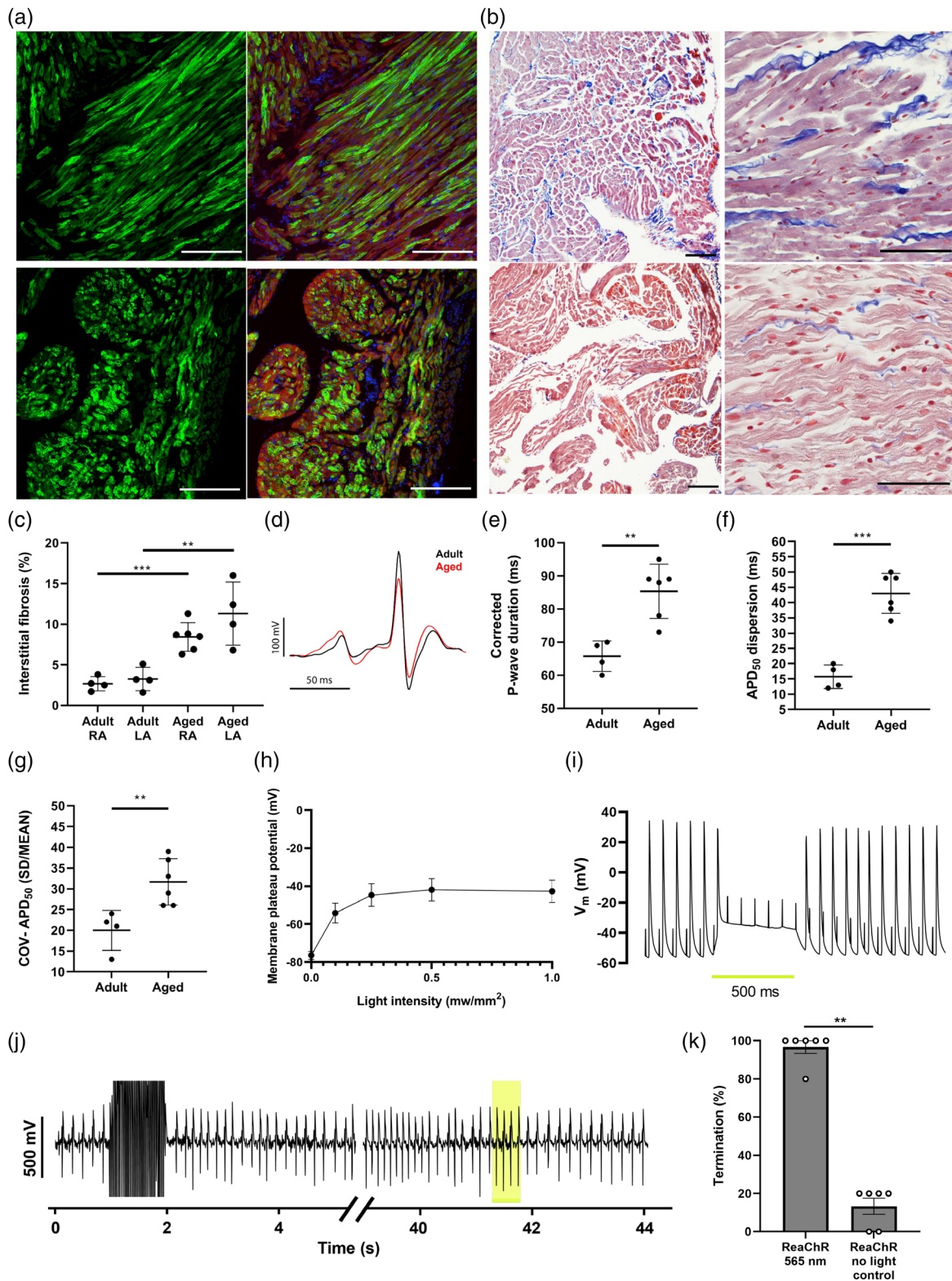
soldered to enameled copper wires with a diameter of 150 μ m. The solder joints and exposed copper wires on the back side of the LED arrangement were then covered by the UV-curable optical polymer described above to ensure electrical insulation and mechanical robustness of the interconnects.

Statistics

Statistical analyses were performed using SPSS Statistics v23.0 (IBM). Comparison of illumination and control groups was performed by the Mann-Whitney *U* test. Other data were compared by using the two-sided Student's *t*-test. Data were expressed as means \pm SD or, for arrhythmia termination efficacies, current densities, and membrane potentials as standard error of the mean (SEM). Differences were considered statistically significant at $p < 0.05$.

Results

AAVVs encoding ReaChR under control of the atrial myocyte-specific human natriuretic peptide precursor A (NPPA) gene promoter (AAV2/9.45.HsNPPA.ReaChR~citricine.SV40pA) [6] were administered by tail vein injections to adult (i.e., 7-week-old) and aged (i.e., 2-year-old) female Wistar rats. Immunohistological analysis of transgene expression in right atrial myocytes showed average transduction rates of 66% \pm 10% ($n = 6$) and 72% \pm 16% ($n = 4$) in aged and adult rats, respectively (Fig. 2A). Average transduction rates of ventricular myocytes were very low, that is, 1.0% \pm 0.7% and 0.8% \pm 0.6% in the aged and adult rats, respectively (Fig. S1). Masson's trichrome staining showed a significant increase in interstitial atrial fibrosis in the RA (8.4% \pm 1.8% vs. 2.7% \pm 0.9%, $p < 0.001$) and left atrium (11.3% \pm 3.9% vs. 3.3% \pm 1.4%, $p = 0.008$) of aged rats compared to adult rats (Fig. 2B,C). Sustained episodes of AF (>30 s) could be readily induced by burst pacing in 75% of aged rats (six out of eight animals), but not in adult rats (zero out of four, $p < 0.001$). Aged rats with successful AF induction were used for further investigation. ECG recordings demonstrated that aged rats had a significantly longer P-wave duration (36.9 \pm 3.6 vs. 24.6 \pm 0.8 ms, $p < 0.001$) and corrected P-wave duration (85.1 \pm 8.3 vs. 65.8 vs. 2.3 ms, $p = 0.002$) than adult rats (Fig. 2D,E). The APD₅₀ as assessed by optical voltage mapping was not significantly different between aged (28.8 \pm 4.8 ms) and adult (24.6 \pm 2.2 ms) rats ($p = 0.104$). However, the dispersion of APD₅₀ (43 \pm 7 ms vs. 20 \pm 7 ms, $p = 0.001$) as well as the coefficient of variation of



APD₅₀ (0.31 ± 0.05 vs. 0.19 ± 0.05 , $p = 0.008$) was significantly greater in aged compared to adult rats (Fig. 2F,G and Fig. S2). Sharp electrode measurements on ReaChR-expressing atrial tissue of aged rats demonstrated strong and sustained depolarization of the membrane potential during 565-nm light stimulation with an average plateau membrane potential of -42.7 ± 14.5 mV ($n = 6$) (Fig. 2H). Furthermore, conduction block due to optogenetic stimulation was demonstrated by the loss of capture during 12-Hz electrical pacing of the atrial tissue (thereby mimicking AF activation frequency in rats) for the entire duration of 565-nm illumination (500 ms, 0.5 mW/mm²) (Fig. 2I). This finding demonstrates that the ReaChR-mediated depolarization of the sarcolemma is effective in the structurally and electrically remodeled atrium.

Next, the feasibility and effectivity of optogenetic AF cardioversion were evaluated in ReaChR-expressing aged rats. To this end, the RA of anesthetized and ventilated rats was visualized by a minithoracotomy of the fourth right intercostal space, followed by rib spreading. Following the induction of AF by electrical burst pacing, the RA was illuminated with three subsequent 500-ms light pulses (565 nm, 1.0 mW/mm²) at 500-ms intervals using an external LED. Optical AF cardioversion was accomplished in all hearts tested ($n = 6$). The effectivity of AF termination after three consecutive light pulses was 97% (SEM 3%), whereas in the no-light control experiments, 13% (SEM 4%) of the arrhythmias were terminated

($p = 0.002$) (Fig. 2J,K and Figs. S3A and S4). This finding demonstrates that the optogenetic cardioversion of AF is feasible in structurally and electrically remodeled atria.

To get an idea of the 565-nm light intensity needed for optogenetic AF cardioversion in humans, we measured to attenuation coefficient of 565-nm light in human atrial myocardium. To this end, left atrial appendages of patients undergoing cardiac surgery were collected and immediately cut with a high-precision vibratome at thicknesses of 0.5, 1, 1.5, and 2 mm (Fig. 1A,B). Because the left atrial appendages were resected following cardiac arrest with high potassium warm blood cardioplegia, the tissue slices still contained blood during the light transmittance experiments. Transmittance of 565-nm light through these samples ($n = 80$ individual measurements on 20 samples derived from 5 patients) was measured and fitted as described above. The calculated attenuation depth was 0.70 mm (corresponding to an attenuation coefficient of 1.42 mm⁻¹), with a good coefficient of determination ($R^2 > 0.87$). Based on a ReaChR activation threshold of 0.5 mW/mm², 565-nm light pulses of 25 mW/mm² are expected to fully penetrate the human atrial wall with an average thickness of 2–2.5 mm [10, 11].

We next evaluated the feasibility of transthoracic optogenetic AF termination in the adult and fully intact rat in order to provide preliminary evidence supporting the possibility of

Fig. 1 Characterization of the aging-related atrial fibrillation (AF) model. (a) representative immunohistological staining of right atrial sections from an aged rat (top panels) and adult rat (bottom panels). Sections are stained for Citrine using antibodies specific for green fluorescent protein (green) and for cardiac troponin I (red) (right panels only). Cell nuclei are stained in blue. Scale bars represent 100 μ m; (b) typical Masson's trichrome staining of the right atrium (RA) of aged rats (top panel) and adult rats (bottom panel) showing increased interstitial fibrosis in the aged rats; (c) quantification of interstitial fibrosis by Masson's trichrome staining of the right and left atrium in aged and adult rats; (d) typical body surface electrocardiographic (ECG) traces of aged (red) and adult (black) rats in overlay showing increased P-wave duration in the aged rat; (e) electrophysiological assessments by body surface ECGs showing a significantly increased corrected P-wave duration in aged rats compared to adult rats; quantification of (f) dispersion of APD₅₀ and (g) coefficient of variation (COV) of APD₅₀ of adult and aged rats as assessed by optical voltage mapping experiments; (h) average membrane plateau potentials measured with the sharp electrode technique at the end of 1-s 565-nm light pulses of varying intensities on atrial tissue derived from red-activatable channelrhodopsin (ReaChR)-transduced aged rats ($n = 6$). Numerical data are represented as mean \pm standard error of the mean (SEM); (i) representative sharp electrode recording of ReaChR-expressing atrial tissue from an aged rat demonstrating 12-Hz electrical pacing before, during, and after 565-nm illumination (500-ms, 1 mW/mm²). Conduction block was demonstrated by the loss of capture during the entire duration of illumination as only artifacts were observed. The pacing to capture interval is temporary prolonged following the cessation of illumination due to the channel-off kinetics of ReaChR; (j) typical body surface ECG trace demonstrating successful *in vivo* optogenetic termination of AF by a single 565-nm light pulse (500 ms, 1 mW/mm²); (k) quantification of optogenetic AF termination in ReaChR-expressing aged rats after three consecutive 565-nm light pulses (1 mW/mm²) of 500 ms at 500-ms intervals, compared to no-light controls. Each dot indicates five termination attempts in one rat ($n = 6$ rats). Error bars represent SEM. ** $p < 0.01$.

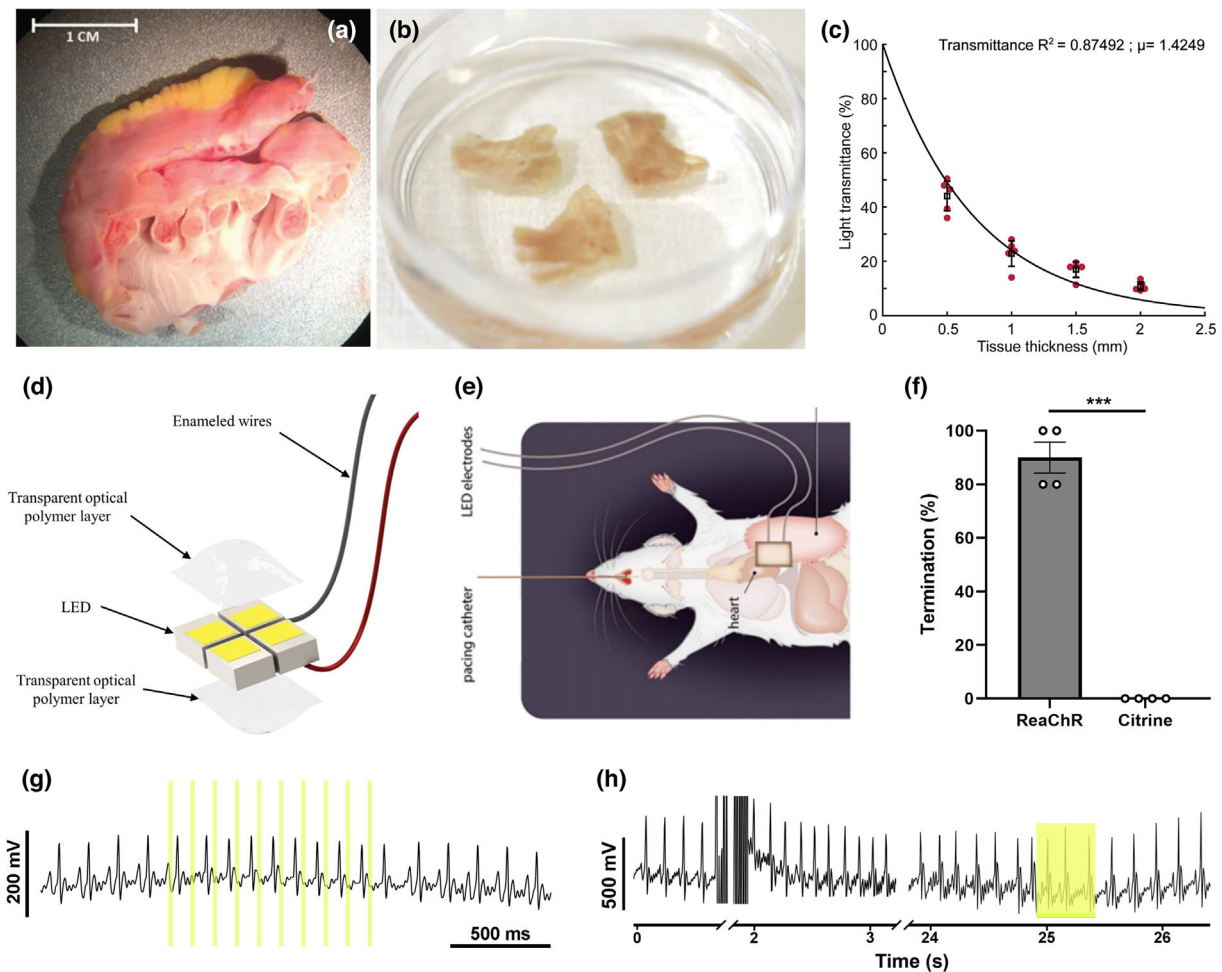


Fig. 2 Light penetration measurements in atrial tissue samples from patients to guide transthoracic optogenetic AF cardioversion in the intact adult rat. (a) fresh left atrial appendage excised from a patient during cardiac surgery; (b) tissue slices of the left atrial appendage cut with a vibratome for light penetration measurements; (c) measurements of 565-nm light penetrance in human atrial tissue slices of 0.5, 1.0, 1.5, and 2.0 mm (4 measurements per thickness of samples from 5 different patients is 80 measurements in total). Experimental data were fitted to a monoexponential decay function; (d) schematic drawing of the light-emitting diode (LED) device used for transthoracic illumination; (e) experimental setup of the transthoracic optogenetic AF cardioversion experiments; (f) quantification of transthoracic optogenetic AF termination in the red-activatable channelrhodopsin (ReaChR)-expressing intact adult rats after three consecutive 565-nm light pulses (25 mW/mm²) of 500 ms at 500-ms intervals, compared to Citrine-expressing control animals. Each dot indicates five termination attempts in one rat (n = 4 rats for both groups). Error bar represents standard error of the mean (SEM). ***p < 0.001; (g) representative body surface electrocardiographic (ECG) trace showing 10-Hz transthoracic optical atrial pacing in the intact adult rat with 10-ms light pulses (565 nm, 25 mW/mm²); (h) representative body surface ECG demonstrating successful optogenetic cardioversion of AF by transthoracic illumination of the intact adult rat (500 ms, 25 mW/mm²).

delivering optogenetic therapy throughout thick tissue segments.

To this end, a custom-made LED device (Fig. 1D) was placed on the shaved skin of the adult rat in the area around the fourth intercostal space. Brief 565-nm light pulses (10 ms) with an irradiance of

25 mW/mm² allowed transthoracic optical pacing of the RA up to 10-Hz in all adult rats tested (n = 4) (Fig. 1G), thereby demonstrating that 565-nm light with an irradiance of 25 mW/mm² could indeed optogenetically stimulate the ReaChR-transduced RA despite being covered by the thoracic wall and other tissues such as lung parenchyma. As

a final experiment, we evaluated the possibility of optogenetic AF cardioversion using the same transthoracic illumination protocol. In order to completely maintain the integrity of the thoracic wall, AF was induced through transesophageal atrial burst pacing (Fig. 1E). Following the induction of AF, three consecutive 565-nm light pulses (25 mW/mm²) of 500 ms at 500-ms intervals resulted in an optical AF cardioversion efficacy of 90% (SEM 6%), whereas the termination efficacy in Citrine-expressing control rats was 0% (SEM 0%) ($p < 0.001$, $n = 4$ for both groups) (Fig. 1F,H and Figs. S3B and S5). These findings may encourage further investigations in larger animal models, advancing the field of cardiac optogenetics and its potential clinical applications.

Discussion

Our results address two important hurdles in the clinical translation of optogenetic AF cardioversion. First, we have demonstrated effective optogenetic AF cardioversion in a clinically relevant model of experimental AF based on aging-related structural and electrical atrial remodeling. This finding represents an important step forward in the clinical translatability of cardiac optogenetic rhythm control for AF as the atrial substrate of the majority of AF patients is based on such remodeling [1]. Moreover, we provided proof that optogenetic excitation and arrhythmia termination of deeper lying tissue is feasible with already available optogenetic and optoelectronic tools.

As this novel therapeutic approach would allow automated and rapid detection and subsequent termination of AF in a shock-free manner, it might especially benefit vital patients with frequent therapy-refractory and highly symptomatic paroxysmal AF. Indeed, AF-related symptoms, morbidity, and adverse effects of medication can have considerable impact on these individuals in particular [12, 10]. In addition, ambulatory rhythm control for AF by optogenetics may also slow down the vicious circle of AF begetting AF by abolishing the stimulus for atrial remodeling, [1, 11] thereby potentially improving the prognosis and quality-of-life of these patients. All these anticipated benefits of acute cardioversion are further supported by the results of recent clinical trials showing that early rhythm control is associated with a lower risk of adverse cardiovascular outcomes in patients with early AF and bring clinical benefit to patients suffering from both AF and heart failure [13, 14].

It is important to note that the calculated irradiance is likely an overestimation, considering that in the current rat model, the excitation light first had to penetrate the thoracic wall before it reached the heart, whereas a possible human application would probably involve direct epicardial illumination. Furthermore, the activation threshold of 0.5 mW/mm² used to mathematically predict the epicardial irradiance needed for optogenetic AF termination incorporated an error margin, as strong and sustained depolarization of the membrane potential could already be achieved with light intensities starting at 0.1 mW/mm² (Fig. 2H). However, given the potential negative impact of sparse or nonuniform transgene expression as well as anatomical and electrophysiological differences between rat and human atrial myocardium, further research (including large animal models) is warranted to validate these irradiance estimations. In addition, it is important to note that our model was based on the assumption that transmural illumination would be an absolute prerequisite for efficient AF termination, which may not be necessary. Interestingly, the use of subthreshold illumination has emerged as a promising strategy to reduce the energy requirements for optogenetic cardiac stimulation [15, 16]. By moderating irradiance, the likelihood of phototoxicity and local heating could be reduced, consequently improving the treatment's safety profile. Additionally, diminished energy requirements may promote the creation of compact, energy-efficient light delivery systems, thereby streamlining the design and extending the longevity of implantable devices for clinical applications.

Our findings therefore strongly suggest that the clinical application of optogenetic cardioversion of AF with a redshifted channelrhodopsin will most likely not be hindered by the average thickness of the human atrial wall. However, optogenetic AF termination could be hindered in patients with thicker than average atrial walls or in patients with atria that are covered by large portions of epicardial fat. To address this potential limitation, patient screening methods could be developed to differentiate potential responders from nonresponders, which may be achieved through modeling patients' atria using cardiac magnetic resonance imaging. It is important to note that it can be expected that progress in the continuously advancing fields of optogenetics and optoelectronics will further enhance the feasibility and effectiveness of optoelectronic

termination of cardiac arrhythmias for clinical application.

The light attenuation depth of 0.70 mm in the present study closely resembles that of Ochs et al. [17] who found a light attenuation depth value of 0.52 mm for 510-nm light based on experimental data by Swartling et al [18]. The small difference can potentially be attributed to the utilization of human left atrial appendage tissue in our study, which may possess distinct optical characteristics compared to the porcine ventricular myocardium used in the research conducted by Swartling et al. In addition, the present study used 565-nm light, which is more redshifted compared to 510-nm used by Swartling et al.

Remaining challenges in the clinical translation of optogenetic AF termination, in addition to adequate and safe transgene expression, concern the implantation of a light device and the potential need to overcome spatially distributed AF driver domains that might not respond to a compact LED array. Rapid advances in optoelectronics have made it possible to develop flexible, thin (<1 mm) and biocompatible LED arrays [19, 20]. Such devices may, for example, be attached to the pericardium or epicardium by a minimally invasive thoroscopic approach, whereas the unit for detection and activation is implanted in a subcutaneous pacemaker pocket. Concurrent epicardial gene painting [6, 21] may ensure that a single minimally invasive procedure suffices for both targeted gene transfer and device implantation. To overcome the potential challenge posed by spatially distributed AF driver domains, a custom-designed LED array could be employed to deliver spatially targeted light stimulation based on the patient's specific atrial anatomy and arrhythmogenic substrate derived. This clinical information could be acquired by cardiac magnetic resonance imaging and advanced AF mapping techniques. This approach could draw inspiration from the established Cox-Maze IV procedure [22], where surgical lesions are created to interrupt AF driver domains. The reversibility and non-traumatizing nature of such "optogenetic ablation lines" offer a potentially less invasive alternative that does not require open heart surgery.

Conclusion

Optogenetic cardioversion is effective in the AF-prone hearts of aged rats and can be achieved

by transthoracic illumination using irradiation levels sufficient for transmural light penetration of human atria. These findings strengthen the translational potential for the development of shock-free anti-arrhythmic device therapy for AF and warrant studies into larger animal models.

Author contributions

Conceptualization; data curation; formal analysis; investigation; methodology; validation; visualization; writing—original draft; writing—review and editing: Emile C. A. Nyns. *Data curation; formal analysis; investigation; methodology; visualization; writing—review and editing:* Vincent Portero and Shanliang Deng. *Investigation; methodology; resources; writing—review and editing:* Tianyi Jin. *Data curation; formal analysis; investigation; methodology; validation; writing—review and editing:* Niels Harlaar. *Investigation; methodology; supervision; writing—review and editing:* Cindy I. Bart. *Data curation; investigation; methodology; resources; writing—review and editing:* Thomas J. van Brakel. *Data curation; formal analysis; investigation; methodology; resources; writing—review and editing:* Meindert Palmen and Jesper Hjortnaes. *Investigation; methodology; supervision; validation; writing—review and editing:* Arti A. Ramkisoensing. *Funding acquisition; resources; supervision; writing—review and editing:* Guo Qi Zhang. *Supervision; writing—review and editing:* René H. Poelma. *Investigation; methodology; supervision; visualization; writing—review and editing:* Balázs Ördög. *Investigation; methodology; resources; supervision; writing—review and editing:* Antoine A. F. de Vries. *Conceptualization; funding acquisition; project administration; resources; supervision; writing—original draft; writing—review and editing:* Daniël A. Pijnappels.

Acknowledgments

This study was supported by European Research Council (starting grant 716509 to D.A.P.). Additional support was provided by The Netherlands Organization for Scientific Research (Vidi grant 91714336 to D.A.P.).

Conflict of interest statement

None of the authors have a conflict of interest to declare.

References

- Lip GY, Tse HF, Lane DA. Atrial fibrillation. *Lancet*. 2012;**379**:648–61.
- Ganesan AN, Shipp NJ, Brooks AG, Kuklik P, Lau DH, Lim HS, et al. Long-term outcomes of catheter ablation of atrial fibrillation: a systematic review and meta-analysis. *J Am Heart Assoc*. 2013;**2**:e004549.
- Arbelo E, Brugada J, Blomstrom-Lundqvist C, Laroche C, Kautzner J, Pokushalov E, et al. Contemporary management of patients undergoing atrial fibrillation ablation: in-hospital and 1-year follow-up findings from the ESC-EHRA atrial fibrillation ablation long-term registry. *Eur Heart J*. 2017;**38**:1303–16.
- Geller JC, Reek S, Timmermans C, Kayser T, Tse HF, Wolpert C, et al. Treatment of atrial fibrillation with an implantable atrial defibrillator—long term results. *Eur Heart J*. 2003;**24**:2083–9.
- Wellens HJ, Lau CP, Luderitz B, Akhtar M, Waldo AL, Camm AJ, et al. Atrioverter: an implantable device for the treatment of atrial fibrillation. *Circulation*. 1998;**98**:1651–6.
- Nyns ECA, Poelma RH, Volkers L, Plomp JJ, Bart CI, Kip AM, et al. An automated hybrid bioelectronic system for autogenous restoration of sinus rhythm in atrial fibrillation. *Sci Transl Med*. 2019;**11**:eaau6447.
- Entcheva E, Kay MW. Cardiac optogenetics: a decade of enlightenment. *Nat Rev Cardiol*. 2021;**18**:349–67.
- Deisseroth K. Optogenetics. *Nat Methods*. 2011;**8**:26–9.
- Nyns ECA, Kip A, Bart CI, Plomp JJ, Zeppenfeld K, Schalij MJ, et al. Optogenetic termination of ventricular arrhythmias in the whole heart: towards biological cardiac rhythm management. *Eur Heart J*. 2017;**38**:2132–6.
- Randolph TC, Simon DN, Thomas L, Allen LA, Fonarow GC, Gersh BJ, et al. Patient factors associated with quality of life in atrial fibrillation. *Am Heart J*. 2016;**182**:135–43.
- Wijffels MC, Kirchhof CJ, Dorland R, Allessie MA. Atrial fibrillation begets atrial fibrillation. A study in awake chronically instrumented goats. *Circulation*. 1995;**92**:1954–68.
- Reynolds MR, Lavelle T, Essebag V, Cohen DJ, Zimetbaum P. Influence of age, sex, and atrial fibrillation recurrence on quality of life outcomes in a population of patients with new-onset atrial fibrillation: the Fibrillation Registry Assessing Costs, Therapies, Adverse events and Lifestyle (FRACTAL) study. *Am Heart J*. 2006;**152**:1097–103.
- Kirchhof P, Camm AJ, Goette A, Brandes A, Eckardt L, Elvan A, et al. Early rhythm-control therapy in patients with atrial fibrillation. *N Engl J Med*. 2020;**383**:1305–16.
- Marrouche NF, Brachmann J, Andresen D, Siebels J, Boersma L, Jordaens L, et al. Catheter ablation for atrial fibrillation with heart failure. *N Engl J Med*. 2018;**378**:417–27.
- Biasci V, Santini L, Marchal GA, Hussaini S, Ferrantini C, Coppini R, et al. Optogenetic manipulation of cardiac electrical dynamics using sub-threshold illumination: dissecting the role of cardiac alternans in terminating rapid rhythms. *Basic Res Cardiol*. 2022;**117**:25.
- Hussaini S, Venkatesan V, Biasci V, Romero Sepúlveda JM, Quiñonez Uribe RA, Sacconi L, et al. Drift and termination of spiral waves in optogenetically modified cardiac tissue at sub-threshold illumination. *Elife*. 2021;**10**:e59954.
- Ochs AR, Karathanos TV, Trayanova NA, Boyle PM. Optogenetic stimulation using anion channelrhodopsin (GtACR1) facilitates termination of reentrant arrhythmias with low light energy requirements: a computational study. *Front Physiol*. 2021;**12**:718622.
- Swartling J, Palsson S, Platonov P, Olsson SB, Andersson-Engels S. Changes in tissue optical properties due to radio-frequency ablation of myocardium. *Med Biol Eng Comput*. 2003;**41**:403–9.
- Park SI, Brenner DS, Shin G, Morgan CD, Copits BA, Chung HU, et al. Soft, stretchable, fully implantable miniaturized optoelectronic systems for wireless optogenetics. *Nat Biotechnol*. 2015;**33**:1280–6.
- Kim RH, Kim DH, Xiao J, Kim BH, Park S-I, Panilaitis B, et al. Waterproof AllnGaP optoelectronics on stretchable substrates with applications in biomedicine and robotics. *Nat Mater*. 2010;**9**:929–37.
- Kikuchi K, McDonald AD, Sasano T, Donahue JK. Targeted modification of atrial electrophysiology by homogeneous transmural atrial gene transfer. *Circulation*. 2005;**111**:264–70.
- Robertson JO, Saint LL, Leidenfrost JE, Damiano RJ Jr. Illustrated techniques for performing the Cox-Maze IV procedure through a right mini-thoracotomy. *Ann Cardiothorac Surg*. 2014;**3**:105–16.

Correspondence: Daniël A. Pijnappels, Laboratory of Experimental Cardiology, Department of Cardiology, Heart Lung Center Leiden, Leiden University Medical Center, Leiden, The Netherlands.
Email: d.a.pijnappels@lumc.nl

Supporting Information

Additional Supporting Information may be found in the online version of this article:

Figure S1: Typical immunostaining of a ReaChR-transduced adult rat displaying both a basal region of the right atrium (RA) and apical region of the right ventricle (RV) for green fluorescent protein (green), cardiac troponin I (red) and cell nuclei (blue). Transgene expression is strong in the RA and almost absent in the RV.

Figure S2: Representative action potential duration at 50% repolarization (APD₅₀) maps for ReaChR-expressing right atria in an aged (A) and adult (B) rat, illustrating enhanced APD dispersion in the aged rat.

Figure S3: Zoomed-in body surface ECG traces showing successful optogenetic termination of atrial fibrillation (AF) by a single 565-nm light pulse in ReaChR-expressing aged (A) and adult (B) rats.

Figure S4: Quantification of optogenetic AF termination in ReaChR-expressing aged rats after 1, 2 and 3 consecutive 565-nm light pulses

(1 mW/mm²) of 500 ms at 500-ms intervals, compared to no-light controls. The middle and left graph show cumulative termination efficacy data. Each dot indicates 5 termination attempts in one rat (n = 6 rats for both groups). Error bars represent the standard error of the mean (SEM).

Figure S5: Quantification of optogenetic AF termination in ReaChR-expressing adult rats after

1, 2 and 3 consecutive 565-nm light pulses (25 mW/mm²) of 500 ms at 500-ms intervals, compared to Citrine-expressing control animals. The middle and left graph show cumulative termination efficacy data. Each dot indicates 5 termination attempts in one rat (n = 4 rats for both groups). Error bars represent SEM. ■